ELSEVIER

Solid State Ionics 131 (2000) 79–96

SOLID STATE IONICS

www.elsevier.com/locate/ssi

Fabrication of thin electrolytes for second-generation solid oxide fuel cells

J. Will, A. Mitterdorfer, C. Kleinlogel, D. Perednis, L.J. Gauckler*

Department of Materials, ETH, Zurich, Sonneggstr. 5, CH-8092 Zürich, Switzerland

Received 15 February 1999; received in revised form 26 April 1999; accepted 5 May 1999

Abstract

This paper reviews different thin-film deposition methods for oxides, especially for stabilized zirconia and compares them with regard to SOFC applications. These methods will be classified into chemical, physical methods and ceramic powder processes. Each method is described with its special technical features and examples of components for fuel cells are given. PVD and CVD methods are specially suited to depositing high-quality films of simple chemical compositions. Liquid droplet methods and ceramic powder processes are more qualified for the deposition of complicated chemical compositions.

Keywords: SOFC; Thin films; Zirconia; PVD; CVD; Liquid precursor methods

1. Introduction

Yttria-stabilized zirconia (YSZ) is the most commonly used electrolyte material for Solid Oxide Fuel Cells (SOFCs) because of its unique combination of properties such as high chemical and thermal stability and pure ionic conductivity over a wide range of conditions. As a result, YSZ today is still the standard electrolyte material in SOFCs. Due to the high operational temperatures (900–1000°C) the material demands upon SOFC components are quite stringent. It would be desirable to lower the operational temperatures (to 700–800°C) so that interconnect, heat exchangers, and structural components may be fabricated from relatively inexpensive metal components [1–6]. One problem associated with lowering the temperature is the increase of the YSZ electrolyte resistivity. This can be overcome by lowering the electrolyte resistance either by decreasing the electrolyte thickness or with alternative materials of higher ionic conductivity at lower temperatures (e.g. Sc-doped zirconia, ceria solid solutions, doped bismuth oxide, etc.). In addition, for both strategies reduced electrode/electrolyte interfacial losses are beneficial.

If the electrolyte thickness is reduced from today's 100–200 μm to a 5–10 μm range a new design for the electrode/electrolyte structure is needed. As the thin electrolyte can no longer be the mechanically supporting component, one of the porous electrodes must take over this function. Then a thin electrolyte film may be deposited on the electrode layer followed by the deposition of the other porous electrode. SOFCs based on thin electrolytes have already

*Corresponding author. Tel.: +41-1-632-5646; fax: +41-1-632-1132.

E-mail address: gauckler@nonmet.mat.ethz.ch (L.J. Gauckler)

0167-2738/00/$ – see front matter
PII: S0167-2738(00)00624-X

been tested and exhibited excellent electrochemical performances (e.g. [7–10]).

We give a survey of the most commonly applied techniques for depositing thin electrolyte films with an emphasis on techniques, which are already used for SOFC processing. Most of the examples are for yttria-stabilized zirconia but are equally applicable to other oxide electrolytes.

2. Deposition of thin ceramic films

2.1. Chemical methods

2.1.1. Chemical vapor deposition techniques

2.1.1.1. General

There are two main chemical deposition techniques such as Chemical Vapor Deposition (CVD) and Electrochemical Vapor Deposition (EVD). Recently few related methods are also proposed and applied. These methods make it possible to control chemical composition and to form a dense film. They are also known to be suitable for mass production.

2.1.1.2. Chemical vapor deposition

CVD is a chemical process in which one or more gaseous precursors form a solid material by means of an activation process. The reactant vapors are (1) transported to the surface of a substrate and (2) adsorbed on the substrate surface where (3) the chemical reaction leads to a solid product for (4) crystal growth.

CVD has been widely used for fabricating microelectronics. Therefore the underlying processes are well understood. Recently several modifications, which might become important for fabricating SOFC components, have been developed. Halogen compounds such as $ZrCl_4$ and YCl_3 [11,12], metal organic compounds such as metal alkoxides [13–15] or β-diketones ([16] and references therein) have been used as precursor materials. Growth rates of the film thickness are in the range of 1–10 $\mu m\,h^{-1}$, depending on the evaporation rate and substrate temperature.

A schematic diagram of a typical CVD apparatus is shown in Fig. 1. Typically fused-silica glass is used as the substrate material which is heated to deposition temperatures of 600–1200°C depending on the reactivity of the precursors.

Chour et al. [15] used butanol containing Zr- and Y-ions as a precursor material and pressed and sintered ceria pellets as substrates. The precursor was heated to 150°C whereas the substrate was heated to about 850°C. The deposition time was 4 h for a film thickness of 5 μm. After annealing at 1300°C for 10 h the YSZ phase in the deposited film became fully crystalline. An Open Cell Voltage (OCV) of 0.93 V at 650°C was reported.

The advantages of the CVD technique consist of producing uniform, pure, reproducible and adherent films at low or high rates. It is particularly useful in the deposition of coating in sites difficult to reach by

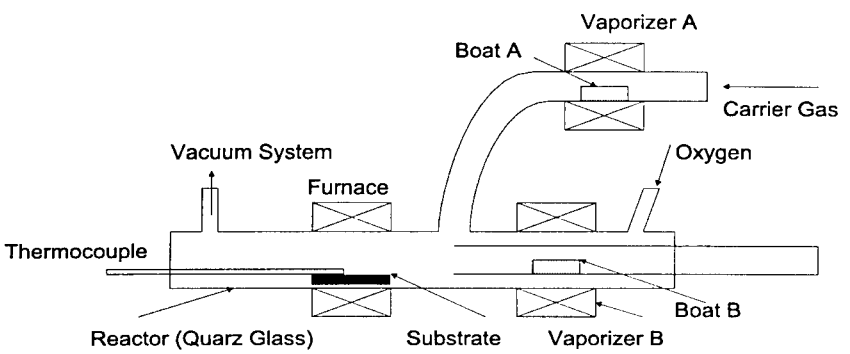

Fig. 1. Schematic diagram of a CVD apparatus for preparation of ZrO_2, Y_2O_3 and ZrO_2–Y_2O_3 films (after [16]).

other deposition techniques. Disadvantages are the high reaction temperature, the presence of corrosive gases (at least for halogenous compounds), and the relatively low deposition rates [17].

2.1.1.3. Electrochemical vapor deposition

EVD is a modified CVD process, originally developed by Westinghouse [18,19]. In these CVD-EVD processes, a porous ceramic substrate divides a reactor into two chambers, of which one is filled with a metal compound reactant and the other with an oxygen source reactant. EVD is a two-step process. The first step involves pore closure by a normal CVD type reaction between the reactant metal chloride vapors and water vapor (or oxygen). Film growth then proceeds due to the presence of an electrochemical potential gradient across the deposited film. In this step oxygen ions formed on the water vapor side of the substrate diffuse through the thin metal oxide layer to the metal chloride side. The oxygen ions react with the metal chloride vapors to form the metal oxide product. The solid product can be deposited as a thin film spreading over the internal pore surface in a desired region across the membrane substrate [20]. A schematic diagram of the basic principles of the CVD/EVD process is given in Fig. 2.

A single component cell, consisting of porous YSZ ceramics with an internally deposited dense film, could be produced at growth rates in the range 2.8–52 $\mu m\, h^{-1}$ [21]. Besides the temperature, the morphology of the substrate pores and the chemical parameters influence growth rates. Detailed models of the EVD process have been proposed [7,22].

Modified EVD methods are vapor-phase-electrolytic deposition (VED) [7,23,24], thermophoresis assisted CVD (TA-CVD) [25,26], a combination of EVD and TA-CVD and chemical aerosol deposition technology (CADT) [27].

Ioroi et al. [28] produced fully dense YSZ electrolytes which were deposited on porous $La_{0.85}Sr_{0.15}MnO_3$ substrates. They used $ZrCl_4$ and YCl_3 vapor mixtures as the metal compound sources and water vapor as the oxygen source. An OCV of 1.04 V was reported for a $LaMnO_3$/YSZ/Ni–YSZ with an EVD layer of YSZ, indicating that there was negligible gas leakage through the electrolyte [29]. Cao et al. [30] obtained thin zirconia layers on porous alumina substrates. $ZrCl_4$ and YCl_3 vapor with a ratio of 10:3 were used. After 40–50 min CVD/EVD a gas-tight YSZ layer was formed with a thickness of 0.5–1.5 μm depending on the experimental conditions. The thickness of the YSZ layer increased with the deposition temperature, e.g. 5 μm at 800°C and 19 μm at 1000°C. Sasaki et al. [31] deposited 18-μm thick YSZ layers on cathode tubes. They reported a power density of 0.8 $W\, cm^{-2}$ with an active area of 1200 mm^2. Thin (2 μm) YSZ layers were deposited on pressed and sintered ceria substrates (20 mm ∅) by Nord-Varhaug et al. [32]. They used $ZrCl_4$ and YCl_3 metal–chloride precursors. The main problem was cracking of the substrate

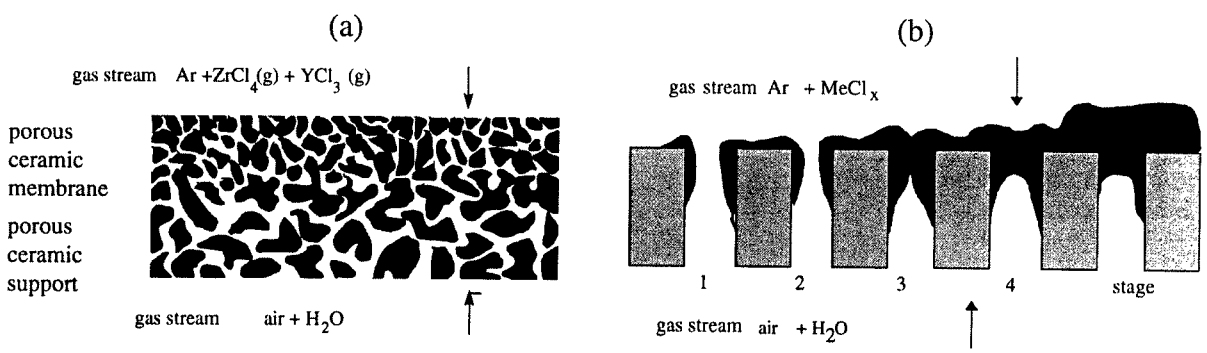

Fig. 2. (a) A schematic diagram of the basic principles of the CVD/EVD processes. (b) Detailed view of the different stages during the CVD/EVD processes in which the solid product is mainly deposited at the chloride side (after [20]).

during heating at 770–950°C, which was probably due to the insufficient mechanical strength of the substrate.

The disadvantages of the EVD process are the high reaction temperature, the presence of corrosive gases, and the relatively low deposition rates. However, EVD is a widely used technique for depositing uniform and gas tight layers of YSZ and interconnect materials for SOFC.

2.1.2. Thin films by the liquid precursor route

2.1.2.1. General

Starting from a molecular precursor, one obtains a hydroxide or oxide network via inorganic polycondensation reactions. For this reason, extremely thin, dense, and well-defined films can be produced. Purity and uniformity are also easy to be controlled by the solution chemistry of the sol–gel process.

Metal alkoxides $M(OR)_n$, where R is usually an alkyl group, are generally the most versatile precursors. Alkoxides are known for almost all transition metals as well as for the rare earth metals [33] and are very reactive towards a reagent such as water. Up to now, zirconia films have been prepared from (1) zirconium propoxide [34–38], (2) zirconium tetrabutoxide [39,40], and (3) from a hydrosol prepared from a zirconium oxychloride solution [41].

2.1.2.2. Sol-gel route

Gelling occurs through the formation of a polymeric network. Fig. 3 shows the two steps of hydrolysis and polymerization by condensation where R is an alkyl group in case of Me = Zr. The desired amount of yttrium is achieved by addition of yttrium nitrate ($Y(NO_3)_3$–nH_2O).

The resulting network structures are strongly influenced by the respective kinetics of the reactions, which in turn depend on many parameters. The sol–gel transition occurs during deposition due to solvent evaporation that accelerates the reaction rates among the precursor oligomers. The desired microstructure is determined by the precursor reactivity and the deposition conditions [43,44]. The substrates are coated either by spin- or dip-coating techniques [45,46]. Once coated, the samples are dried at room temperature and heat treated for densification and

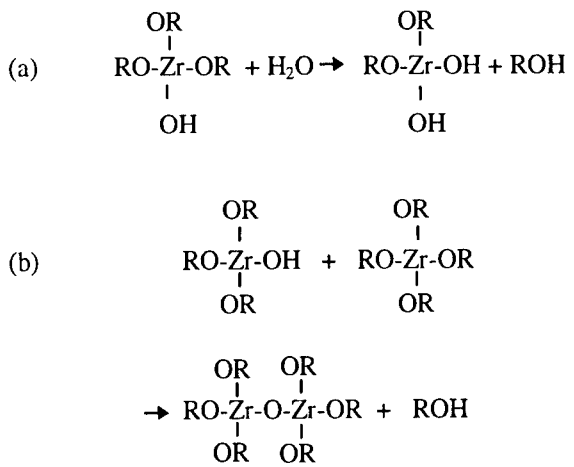

Fig. 3. Hydrolysis reaction and polymerization using the condensation mechanism [42].

crystallization of the film. The process of coating and drying/heating is usually repeated until the appropriate thickness is obtained. Sol-gel derived films, due to their fine structure and high density, can be sintered at much lower temperatures than those films made by conventional ceramic powder processing.

Alternatively the dilution of reactants can also influence the gelling time and finally the gel structure, as expected from simple laws of chemical kinetics. YSZ films described by Kueper et al. [38] were formed using a well-defined relative humidity during the deposition. They were about 0.2 mm thick and uncracked. Peshev et al. [36] showed that good-quality YSZ films of 120–150 nm thickness can be easily deposited on various smooth substrates (Si wafer, sapphire, optical silica glass, and alumina) using a sol–gel technique using zirconium propoxide ($Zr(O–C_3H_7)_4$) and yttrium isopropoxide ($Y(CH_3)_2CHO$) in isopropanol with ethyl aceto-acetate ($CH_3COCH_2CO_2C_2H_5$) as chelating agent. By repeating the deposition steps the film thickness can be increased. Mehta et al. [47] deposited thin layers of YSZ with 11 mol.% Y_2O_3 on sintered disks of Gd-doped ceria electrolyte using spin coating alkoxide solutions. Dense films were obtained by this method on polished ceria substrates. After heat-treatment at 600°C the zirconia film thickness was 1–3 μm. At 600°C an OCV of 0.85 V was achieved after repeating the coating process three times. Nam et al. [48] used the sol–gel method combined with the

spin-coating technique to fabricate thin zirconia layers on pressed and sintered ceria electrolytes with a diameter up to 50 mm. The polymeric YSZ sol was synthesized using the partial hydrolysis of Zr–*n*-butoxide. Acetic and nitric acid were used as chelating agent and catalyst, respectively. Thin films of YSZ were deposited on the ceria substrates by spin coating of the sol at a spin rate of 2000 rpm for 20 s. After drying, the sample was heat-treated at 600°C. The coating, drying and heat treatment processes were repeated until the thickness of the coated film reached 2 μm. The sample was finally sintered at 1400°C for 2 h. Anderson et al. developed a solution-deposition technique [49,50]. The starting solution was prepared from zirconyl chloride hydrate and yttrium nitrate hydrate. A spin coating technique was used to form films onto either LSCF or LSM. Multiple coatings with drying and a subsequent heat treatment at 400–1000°C after each coating produced thicker films. The film thickness increased with increasing viscosity of the solution and decreasing spinning rate and time. Films of 0.1–0.3 μm thickness for each coating could be obtained with a spinning speeds of 2000 to 3000 rpm and a viscosity between 90 and 190 cp. Reiichi et al. [51] produced a composite electrolyte consisting of a zirconia film about 1 μm thick deposited using the sol–gel method onto a Ni–cermet substrate. A corresponding cell operated with moist H_2 and O_2 exhibited an OCV of 1.0 V at 800°C.

2.1.2.3. Spray pyrolysis method

A schematic diagram of a typical spray pyrolysis setup is shown in Fig. 4. A metal salt solution (usually aqueous or alcoholic) is sprayed onto a hot substrate to obtain the corresponding metal oxide films. Sprayed droplets reaching the substrate surface undergo pyrolytic (endothermic) decomposition. The substrate provides the thermal energy for the decomposition. A sufficiently high force applied to the surface of a liquid in the nozzle causes the emission of droplets. Three different groups of atomizers were employed for the generation of the spray: blast (using a stream of gas at high velocity) [52], ultrasonic (using an ultrasonic irradiation) [53,54] and electrostatic [55] (using a high voltage). The technique of atomization determines the droplet size distribution, efficiency and spray angle. The electrostatic atomization technique leads to almost monodispersed drops and also to finer droplets than can be produced by other techniques. Overspray is reduced due to the charged droplets, therefore the electrostatic atomization increases the deposition efficiency.

Spray pyrolysis usually has deposition rates of 1–5 $\mu m\,h^{-1}$. Choy et al. [52] however, report deposition rates of YSZ on porous LSM substrates as high as 60 $\mu m\,h^{-1}$. Dense 50-μm thick YSZ films were also deposited at 650°C. Thin films of calcia-stabilized zirconia (CSZ) were deposited on a LSM porous substrate by spray pyrolysis [56]. The OCV of the cell consisting of 33-μm thick CSZ film, LSM cathode, and Ni–YSZ cermet anode was 0.96 V and the maximum power density was 0.5 $W\,cm^{-2}$ at 1000°C. Chen et al. [55] deposited YSZ films on GCO substrates. Dense thin YSZ layers of about 1 μm were only found under the several cracked and porous top layers. Such composite electrolyte structures are interesting for intermediate-temperature

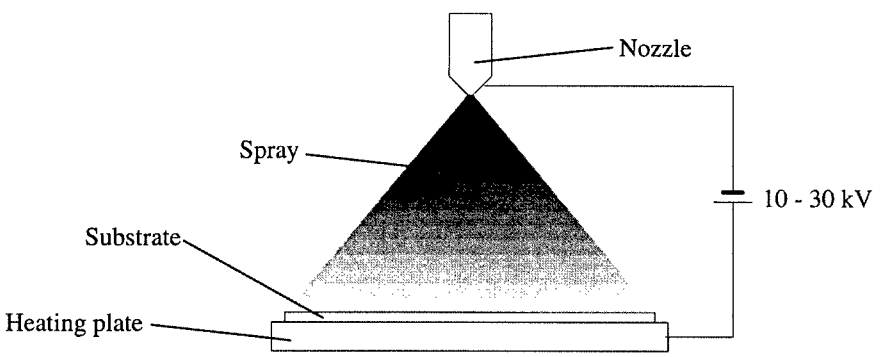

Fig. 4. A schematic diagram of a typical spray pyrolysis setup.

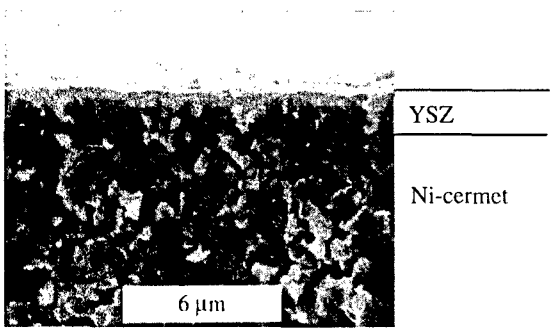

Fig. 5. Cross-section of a YSZ film deposited on a porous Ni–cermet substrate [57].

SOFC, because the YSZ-coated ceria electrolytes were found to exhibit a higher open-circuit voltage compared to uncoated ceria [56]. Fig. 5 shows the microstructure of a YSZ layer sprayed on a porous substrate [57]. The zirconia layer was amorphous before heat-treatment. After a treatment at 600°C polycrystalline YSZ could be obtained.

2.2. Physical methods

2.2.1. Thermal spray technology

2.2.1.1. General

Thermal spraying is a generic term for thick (100–500 μm) overlay processes in which coating material is heated in a gaseous medium and projected at high velocity onto a component surface [58]. These processes are probably less applicable to produce thin electrolytes. They may be useful however for the deposition of porous electrodes [59] or electrolytes other than conventional YSZ, e.g. ceria or bismuth oxide, which show significant higher ionic conductivity at intermediate temperatures.

2.2.1.2. Conventional spray techniques

Various techniques can be used depending on material and desired coating performance. These include flame spraying (FS), air plasma spraying (APS), low-pressure plasma spraying (LPPS), detonation flame spraying (DFS), electric arc spraying (EAS), and more recently high-velocity oxyfuel (HVOF) spraying. Common to spraying processes are the high temperatures involved, the rapid quenching of the melted ceramic particles on the cold substrate during deposition, and the thermal treatments required to improve the film density (and therefore to reduce the pore volume). All of them can affect the structure and modify the electrical properties of sprayed films with respect to sintered materials. Commercially available ZrO_2 and Y_2O_3 powders are used. They are manufactured by conventional processing techniques [60] such as mixing grinding, heating, and granulation [61,62].

Scagliotti et al. [63] produced plasma-sprayed yttria-stabilized zirconia films, which were dense, with a few large voids but no open porosity after high-temperature (>2000 K) vacuum sintering and air annealing. The zirconia films were fully stabilized in the cubic phase with bulk conductivity and an activation energy similar to those of single crystals with the same composition. Varcalle et al. [60] found that only the powder feed rate and the traverse rate were significant factors affecting the deposition thickness. The key to maximize the economics of the zirconia coating deposition is to optimize the powder feed rate and the traverse rate. Injection angle, standoff distance, traverse rate and secondary flow all have a significant contribution to the variation in porosity. Thus, further study concerning porosity should be concentrated on these factors. Arai et al. [64,65] sprayed YSZ powder on porous electrode substrates consisting of LSM and Ni–cermet. The substrates could endure the thermal shock during the plasma-spraying process. The films were gas-tight, but still contained microcracks. Nicoll et al. [66] gave a survey of the critical parameters involved in VPS such as powder chemistry and morphology. Schiller et al. [67] manufactured a multilayer in one consecutive spray process. They produced an entirely plasma sprayed PEN (Positive electrode/Electrolyte/Negative electrode) consisting of the anode, electrolyte and cathode layer on a Ni felt. The anode, electrolyte and cathode layers had a thickness of 80, 70 and 100 μm, respectively. By applying optimized spray parameters with appropriate torches and nozzles, complex coatings, such as graded cermet layers, with a desired material and porosity can be realized. Aihara et al. [68] plasma-sprayed YSZ films on MnO_2 pre-coated lanthanum manganite substrates which were sintered at 1400°C. However, the thickness of the zirconia layer with 100 μm is rather high

and the sample size (15 mm ∅) is relatively small. An OCV of 1.05 V was measured at 1000°C. Henne [69] produced a whole PEN structure by vacuum plasma spraying in one consecutive process. Ni-felts, embedded in a porous sprayed Ni-matrix, served as base compounds and simultaneously as anodic electric contacts. The next layer consists of the Ni/ZrO_2 with gradually reduced content of Ni and decreasing porosity and pore size toward the dense and gas tight zirconia layer. The Perovskite layer was sprayed on the zirconia layer. Power densities of 230 mW cm^{-2} at an operational temperature of 910°C could be obtained. Gruner [70] also used the VPS method to produce a complete PEN-structure in a single run. The power density was 200 mW cm^{-2} at 910°C for an active area of 4.5 cm^2 with an electrolyte thickness of 250 μm.

2.2.2. Laser deposition techniques

2.2.2.1. General

Laser deposition has become a new and important technique for depositing thin films of a variety of materials. The ability to deposit almost any material, preserve the stoichiometry of multicomponent compounds and to carry out reactive deposition has finally been recognized and renewed the interest in this technology [71]. YZP (Yttria-stabilized Zirconia Polycrystals) thin films deposited by pulsed laser deposition have been known for a couple of years, since the availability of high-energy pulsed UV lasers.

2.2.2.2. Pulsed laser deposition (PLD)

The basic set-up of a laser ablation equipment is shown in Fig. 6. The process involves a number of complex interactions among the process variables such as wavelength, power density, background gas, pressure, target composition, substrate–target distance, substrate temperature, substrate bias and gas–surface interactions. PLD requires temperatures of around 500 to 700°C to deposit high-quality crystalline films. It is relatively easy to produce multilayers by substitution of targets into the path of the laser beam. In a commercial setup the possibility of time-sharing a laser among a number of deposition/analysis chambers has been considered. One of the advantages of PLD is the potential for scaling up to production size and volume.

Murray et al. [72] used the frequency-doubled output (0.53 mm), of a Q-switched Nd:YAG laser (15 ns pulses at 5 Hz) to evaporate the YSZ target. The growth rate was relatively low (0.15–0.5 μm h^{-1}) because of the target's low quantum yield to 0.53-mm YAG radiation. Kokai et al. [73,74] deposited YSZ thin films by XeCl excimer laser ablation using a bulk YSZ target (20 ns pulses, 0.308 mm at 10 Hz). The deposition (1 μm h^{-1}) of dense

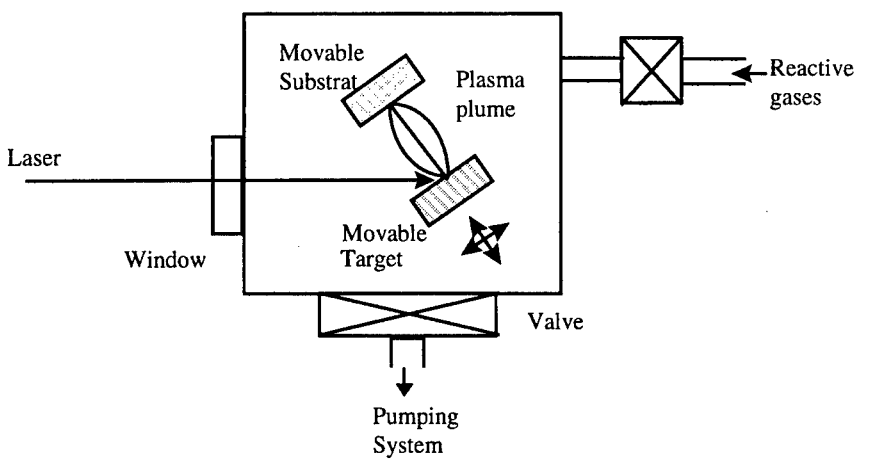

Fig. 6. Laser ablation equipment for deposition of advanced materials. The laser pulse passes through a window and impinges on the target material which is vaporized and deposited on the substrate in the form of a thin film [71].

YSZ films (0.5–2 μm) with excellent adhesive properties at 800°C was demonstrated on a CeO_2–Sm_2O_3 substrate maintained at 500°C in O_2 atmosphere. The post-deposition annealing of the YSZ film at 800°C resulted in the promotion of crystallinity. The film consisted of a cubic phase grown with a predominance of (200) orientation.

Surface melting (sealing) is a potential method to produce shiny surfaces of low roughness on a plasma-sprayed zirconia coating. But the problems of cracks, depressions, islands, etc. have not yet been solved [75,76].

2.2.2.3. Laser spraying

The laser spraying technique uses a carbon dioxide laser beam which is passed parallel to the substrate [77,78]. Thick YSZ layers of 60–150 μm were deposited. The powder, which is supplied through a special device (sometimes with the help of a carrier gas) melts in the laser beam and adheres to the substrate. The process is controlled by the laser power density, substrate temperature, reaction or carrier gases and reactor pressure.

2.2.3. PVD techniques

2.2.3.1. General

Physical vapor deposition (PVD) is a generic term for a variety of sputtering techniques. Radio frequency (RF) sputtering has been most widely used for YSZ film deposition in the production of SOFCs [79–81]. However, YSZ deposition rates during RF sputtering are generally relatively low due to the low sputtering yield of YSZ (0.25 μm h^{-1}). A schematic diagram of the apparatus is shown in Fig. 7. Reactive magnetron sputtering allows much higher deposition rates (2.5 μm h^{-1}) because of the higher sputtering yield. In addition, magnetron sputtering provides ion irradiation of the film during deposition, which has been shown to be crucial for obtaining high-density films at low temperature [82].

The ion-beam-assisted deposition (IBAD) techniques [83] resemble the reactive magnetron sputtering technique, where an ion beam and a reactive background gas are the primary components for producing the coating. Thin films may also be deposited by vacuum evaporation of a target using an electron beam heating device [84]. The deposition rates achieved are in general two orders of magnitude higher than for the above-mentioned methods (typically 1 μm min^{-1}).

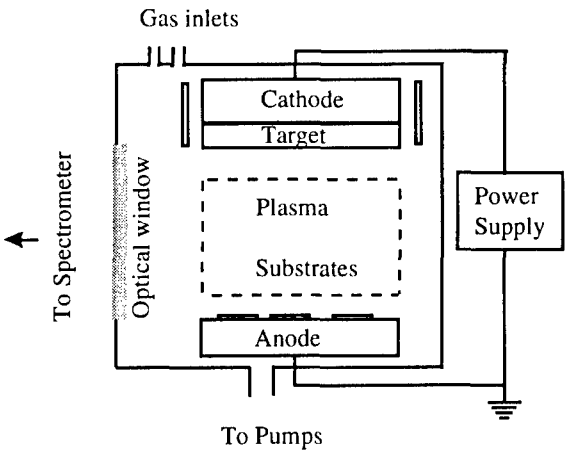

Fig. 7. RF-diode sputtering deposition apparatus [71].

2.2.3.2. RF-sputtering technique

Sputtering deposition is widely used to grow alloy and component films in which one or more of the constituent elements are volatile. Low-defect-density films of high-melting-point materials can be grown on unheated substrates because phase formation is primarily governed by kinetics, rather than by thermodynamics.

An evacuated chamber is filled with the sputtering gas. A large negative voltage is applied to the cathode. The sputtering gas forms a self-sustained glow discharge. RF-excitation allows use of a non-conducting target or a metal target surface that has become oxidized. Physical sputtering of the target occurs when positive ions from the plasma that are accelerated across the dark space strike the target surface. Material, which is ejected by a momentum transfer process, is mostly uncharged and moves between the electrodes where it becomes thermalized and condenses on any surface. A metal oxide film is grown by sputtering a metal target in a discharge containing oxygen, usually in conjunction with a noble gas. The sputtering process can dissociate an oxidized target surface. Therefore, the sputtered flux may consist of both metal atoms and metal oxide molecules. The metal, metal oxide and oxygen species that arrive at the substrate are adsorbed and ultimately incorporated into stable nuclei to form a

continuous film. These processes are the major factors determining film chemistry, short-range atom order, crystallography and microstructure.

Ceramic thin films may be deposited on various substrate materials. During sputtering the substrate temperature usually does not exceed 70°C. Annealing may be carried out after sputtering deposition both in order to repair damage from sputtering and to study effects of annealing temperature on the structural and electrical properties. Typical film growth rates are 0.15–0.5 $\mu m\,h^{-1}$.

YSZ films deposited on various substrates were found to be of cubic structure [69,70]. Annealing treatment at 800–900°C led to cracking of the YSZ films. However, thermal post-treatment at 1500°C improved the quality of the film by crack healing [69]. The authors found a severely cracked film, (after heating to $T = 900$°C) but no delimitation. Stress in the YSZ film is induced by differences in thermal expansion coefficients of YSZ ($\alpha = 10.5 \times 10^{-6}\,K^{-1}$) and CeO_2 ($\alpha = 12.5 \times 10^{-6}\,K^{-1}$). As the substrate is much thicker than the film, it is to be expected that the film will be under a large (biaxial) tensile stress at heating. The higher the temperature of the treatment, the greater was the crack density [85]. The problem of high tensile stress in thin films due to heat treatment may be avoided by introducing compressive stress in the film during or after sputtering.

A correlation between deposition rate and RF power was demonstrated by Charpentier et al. [86]. They deposited zirconia films on to dense nickel or silica substrates. Growth rates of 0.25 $\mu m\,h^{-1}$, 0.3 $\mu m\,h^{-1}$, and 0.5 $\mu m\,h^{-1}$ for 400, 500 and 800 W, respectively, were obtained. They observed that heating of the substrate at 500°C results in a surface without apparent cracks compared to a situation without heating. Gao et al. [87] deposited zirconia thin films of about 0.5 μm on glass and silicon substrates. The film growth rate increased approximately linearly with power between 300 and 500 W but did not change with argon gas flow-rate or pressure. After deposition, the films were annealed in air at 500–700°C.

2.2.3.3. Reactive DC current magnetron sputtering

This method was first used by Konushi [88] to deposit YSZ for epitaxial growth. The principles for deposition of electrolyte films or Ag–cermets are straightforward. Deposition is initiated, after starting the oxygen flow by rotating the substrate into position over the target. The steady-state temperature of the substrate reaches 70°C during deposition. The substrate may be heated. By changing the sputter sources and sputter parameters a wide variety of different compositions and structures with specific properties may be obtained. Film deposition rates mainly depend on oxygen flow-rate. The decrease in deposition rate is attributed to the formation of oxides on the target surfaces, which are generally characterized by a much lower sputtering yield than the metals.

Jones [89] used this method to deposit ZrO_2 with a high deposition rate up to 9 $\mu m\,h^{-1}$. Wang and Barnett were successful in producing fully dense films at a deposition temperature of 350°C [90,91]. Their Ag–YSZ cermets had a high conductivity and a low overpotential during operation. Multilayer electrolytes for SOFCs were operated at temperatures around 750°C. Three-layer cells consisting of 1-μm thick Ag–YSZ cermet, a 14–20-μm thick YSZ electrolyte, and a 1–2.5-μm thick Ni–YSZ cermet were deposited on polished alumina disks. The cell exhibited an OCV of 0.8 V, less than the expected 1.1 V at 750°C and a maximum power density of 35 $mW\,cm^{-2}$.

Charpentier et al. [86] deposited a 4-μm thick YSZ film on a porous nickel substrate at 500°C. They found that the porosity of the substrate had a crucial influence on the quality of the films. The pore size of the substrate must be limited to 2 μm. The maximum deposition thickness which could be reached in one step is 4 μm. Honegger et al. [92] deposited a bilayer of YSZ (4 μm)/CYO (Y_2O_3 doped ceria) (1 μm) electrolytes on anode substrates (35 mm ∅). The cell showed maximum power densities of up to 1 $W\,cm^{-2}$ at 720°C. OCV values of 0.98 V were obtained at 700°C. The low OCV values were attributed to leakage of oxygen from the cathode side to the anode chamber. The reported value of the deposition rate was 5 $\mu m\,h^{-1}$ for YSZ. Badwal et al. [93] measured a power density of 350 $mW\,cm^{-1}$ at 800°C for a cell (17 mm ∅) with YSZ thin electrolytes.

Kleinlogel et al. [94] used this method to deposit CYO–YSZ bilayers on cathode substrates (50 mm ∅). Thin 10 mol.% yttria-doped ceria solid solutions and 8 mol.% yttria-stabilized zirconia bilayers were

deposited on porous cathode substrates using DC magnetron sputtering in O_2–Ar plasmas using CeY-alloy and ZrY-alloy targets. Dense, microcolumnar film structures were already obtained at substrate temperatures as low as 250°C during deposition. Cell tests were performed using air as the oxidant and a humidified mixture of 70% N_2/30% H_2 as the fuel. An open-circuit voltage of 1.06 V was obtained at 700°C, indicating that the electronic conduction of the CYO layer was blocked by the YSZ layer. A maximum power output of 230 mW cm^{-2} (0.4 V 600 mA cm^{-2}) has been achieved. Fig. 8 shows a cross-sectional view of the sputtered electrolyte bilayer.

2.3. Ceramic powder processing methods

2.3.1. Thick film techniques

2.3.1.1. General

The tape casting, screen printing, and bulk sintering techniques have been extensively used for preparing electrolytes of a few tens of microns to >200 μm thickness. Although satisfactory results with SOFC prepared with the techniques described previously have been obtained at high temperatures (>950°C), the upscaling of component size still has remained as a major problem [95,96]. Tape-casting and screen-printing techniques could be potential candidates for producing electrolytes with diameters of 10–30 mm thicknesses in an inexpensive way.

2.3.1.2. Screen-printing

A highly viscous paste consisting of a mixture of ceramic powder, organic binder and plasticizer is forced through the open meshes of a screen using a squeegee. Parameters such as grain size, grain form, surface properties and packing density of the powder have to be optimized. The screen-printed films are dried and sintered at high temperatures. The sintering temperature, time and atmosphere are also important for good-quality films [97].

There are few publications on screen-printed dense films of stabilized zirconia. Bauza et al. [98] produced both porous and dense films, with a high ratio of electrode area to thickness which can be 1–2 orders of magnitude higher than that of conventional disks (pressed and sintered). Porosity arises mainly due to the agglomeration of the small particles in commercial powders. It was shown by Gödickemeier [99] (see Fig. 9) that electrolytes can be screen-printed on porous or dense substrates (Ni–YSZ cermets). More recently, Cassidy used the screen-printing technique as a method to deposit a zirconia layer onto a tape-cast anode support. The green anode–electrolyte bilayer was sintered resulting in an electrolyte thickness of around 8 μm. An OCV of 0.94 V has been achieved [100,101].

2.3.1.3. Tape casting

Starting from ceramic powders, green tapes are produced which may be then cut into different

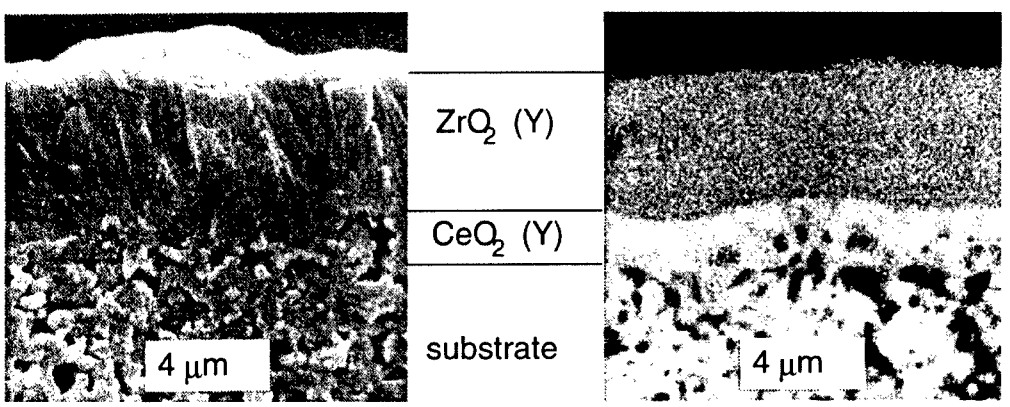

Fig. 8. SEM picture (left) and elemental analysis (right) of an electrolyte bilayer deposited via DC sputtering on top of a porous cathode substrate. It consists of a 1-μm thick CeO_2 (Y) chemical compatibility layer and a 4-μm thick ZrO_2 (Y) electrolyte layer [94].

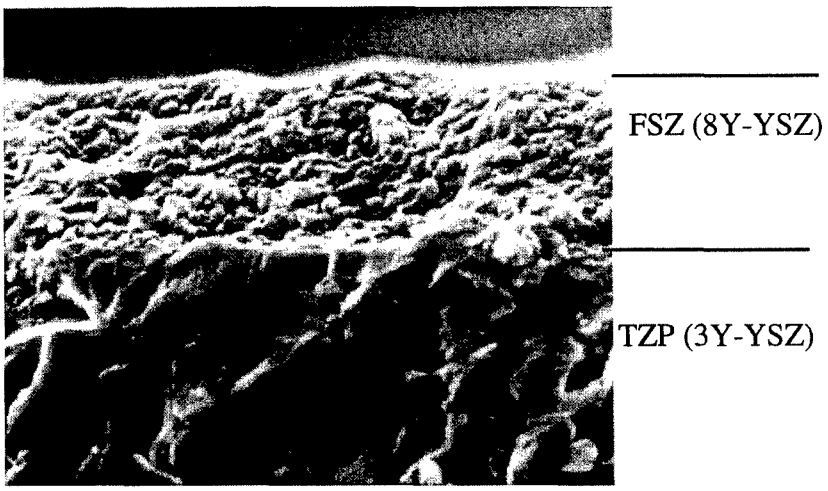

Fig. 9. SEM micrograph of a zirconia layer processed via screen-printing. Fracture surface: 8Y–YSZ layer on a 3Y–YSZ substrate [99].

shapes. The preparation of the slurry for this technique is similar to that of the paste for the screen printing method, and is achieved by conventional methods. By casting the slurry directly onto the joining substrate, unnecessary handling steps may be avoided and less binder and plasticizer have to be added [102]. Cermet fabrication (25–100 μm) is also possible by tape casting [103].

Tape casting has been developed to produce large-area, thin, flat ceramic layers for the monolithic and planar SOFC. Van Berkel et al. [104] used a multilayer tape casting technique, with which an electrode layer is tape-cast on top of a green thin electrode layer. A 50×50 mm^2 bilayer of 10 μm zirconia on a YSZ/Ni-anode tape could be manufactured. Ihringer et al. [105] used a water-based tape casting method and produced 0.6–10 μm YSZ layers which were cast on 200–250 μm NiO/YSZ anode substrates and co-sintered at 1350°C. After sintering, the complementary cathode was deposited. The cells (31 mm ∅) exhibited a power density of 580 mW cm^{-2} with an OCV of 1.01 V at 760°C. Will [106] produced thin zirconia tapes and laminated them at 50°C with a separately produced green Ni–cermet tape. The resulting microstructure after sintering of the bilayer is shown in Fig. 10. The closed porosity of the zirconia layer was characterized by isolated round holes with diameters of 3–5 μm. They were probably formed due to the high organic content in the green tape.

2.3.1.4. Slurry coating technique

Thin film electrolytes may be fabricated also by the slurry coating method [60,95]. A water suspension with a small amount (< 5 wt.% of YSZ) is used to coat a substrate. The thin films were then dried at room temperature, pre-heated at elevated temperatures, and finally sintered. This cycle is normally repeated 5–10 times. Using an ethanol suspension of YSZ [95] may significantly shorten the drying step. Normally repeated coating may eliminate cracks. Thin and dense films with no observable crack were produced by Arai et al. [107]. Aizawa et al. [108] used the slurry coating technique to deposit a 20–30-μm thick zirconia film on tubular cathode substrates. The films were dense and such cells exhibited an OCV close to the theoretical value. Nam et al. [109] deposited YSZ films on pressed porous NiO/YSZ substrates. A 12 wt.% YSZ slurry was prepared and dip-coated on one side of the substrate. The film-coated anode was sintered at 1150°C for 1 h. The dipping–heating cycle was repeated to reach the desired thickness of the electrolyte followed by a final sintering step at 1430°C for 4 h. With two coatings the final electrolyte thickness was 10 μm. An YSZ suspension was deposited on partially

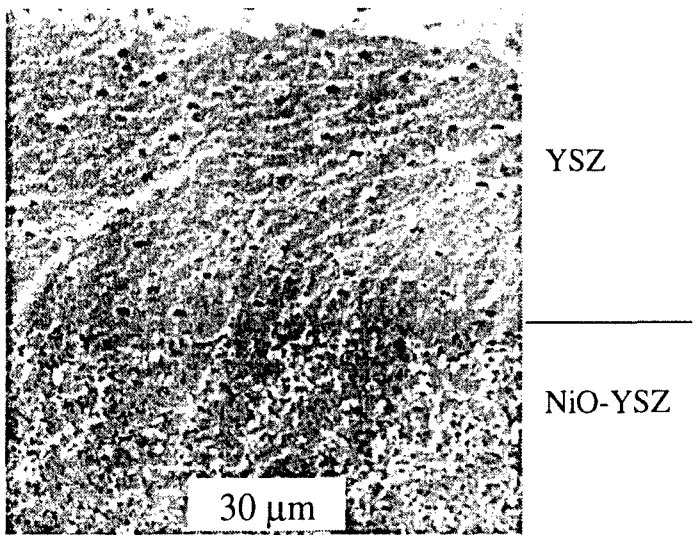

Fig. 10. SEM micrograph of a zirconia layer fabricated via transfer printing after sintering. Fracture surface: zirconia on top, Ni–cermet below [106].

sintered anode or cathode substrates by Visco and Souza [8,110,111]. The substrates (25 mm ∅) were pre-fired to the extent that the shrinkage profile of the substrate exceeds that of the YSZ film. In this way, the film is under compression rather than tension while sintering, and highly dense, crack-free films, 4–10 μm thick, were deposited in a single step. The cell exhibited a power output of 650 mW cm^{-2} at 800°C using a sputtered layer of Pt. Ni–YSZ/YSZ/LSM cells built with this technique exhibited an exceptionally high power density of 1930 mW cm^{-2} at 800°C. Will [106] coated porous pre-sintered Ni–cermet tapes with zirconia suspensions. After drying, the coating was repeated. Fig. 11 shows the resulting microstructure after repeating the coating process five times followed by sintering of the bilayer. The zirconia layer (5 μm) adhered very well to the anodic substrate. Some of the zirconia

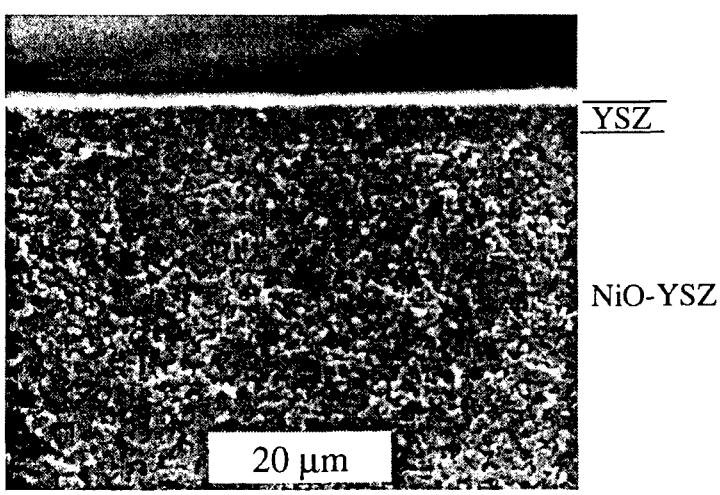

Fig. 11. SEM micrograph of a zirconia layer processed via slurry coating after sintering. The coating–drying cycle was repeated five times. Fracture surface: zirconia on top, Ni–cermet substrate below [106].

was deposited inside the porous substrate, which results in a very good mechanical interlocking.

2.3.1.5. Slip casting

Thick films may also be prepared using the slip casting process [112,113]. The slip (1:3 vol.% powder:water) was on a porous mold and the excess slurry was drained. After drying, the green compact was removed from the mold and then sintered. The density of the sintered samples was $<95\%$ and a small number of pores could be observed in SEM.

2.3.1.6. Filter pressing

The efficiency of the slip casting process normally is rather low. Using a low vacuum may enhance it. Förthmann et al. [114] coated gastight zirconia layers on presintered porous anode substrates with sizes up to 100×100 mm. Coating was performed in two steps: first, closing the open surface pores of the substrate using a 0.15–1.5 μm interlayer consisting of YSZ/NiO, and, second, preparing a 15–20 μm electrolyte layer by using a pure YSZ suspension. The anode substrate/electrolyte unit was subsequently sintered at 1500°C. After deposition of the cathode the cells exhibited a current density of 430 mW cm^{-2} at 800°C. Cells with a 15-μm thick electrolyte layer yield power densities of 230 W cm^{-2} at 750°C [1].

2.3.2. Thin film techniques

2.3.2.1. General

Recently, tape calendering and electrophoretic deposition techniques were applied to produce YSZ thin film electrolytes. Transfer printing is a new method for high-tech ceramics, however, like the other two methods, transfer printing is already known from conventional ceramic processing techniques.

2.3.2.2. Tape calendering

The process involves squeezing a softened thermoplastic polymer/ceramic powder mixture between two rollers to produce a continuous sheet of material. Individual sheets can be calendered and joined to form the multilayer tapes required for SOFCs. Tape calendering of YSZ ceramics was first successfully applied by Minh et al. [9,10] for the production of monolithic and flat plate SOFCs. Minh et al. produced thin (1–10 μm) zirconia electrolyte layers on porous Ni–YSZ cermet supports. Flat plate SOFCs with sizes of 100×100 mm^2 were operated at 600 to 800°C with a platinum paint cathode. A power density of 0.27 W cm^{-1} was achieved at 800°C. The OCV of the cell was 1.1 V, close to the theoretical value.

2.3.2.3. Electrophoretic deposition (EPD)

This technique is one of the colloidal processes in ceramic production and has advantages of short formation time, little restriction of the shape of substrate, and suitability for mass production. In EPD, charged powder particles are deposited from a suspension onto a metallic electrode or a conductive substrate by the application of a DC electric field. The rate of deposition is controllable via the applied potential and can be very fast (1 mm min^{-1}) [115]. Because the green coating contains few or no organics, no burnout procedures are required, and a deposit can be formed on the outside and/or the inside of the electrode. Various kinds of solvents have been applied. Ishihara et al. produced dense YSZ films with a uniform thickness using acetylacetone as solvent. Zirconia films were deposited on cathodic and anodic substrates with electroless plated Pt as anode or cathode [116]. The open-circuit voltage and the maximum power density achieved were 1.03 V and 1.84 W cm^{-2} (1000°C), respectively. The thickness of the YSZ films can be controlled easily by the time and applied voltage. Hruschka [117] and Will [106] deposited zirconia films on pressed or tape-cast anodic substrates with diameters of up to 120 mm. An open-circuit voltage of 0.9 V at 700°C and a power density of 200 mW cm^{-2} were reported. Fig. 12 shows a cross-section of a sintered EPD-derived zirconia layer. The substrate for the deposition was a tape cast Ni–cermet. After co-sintering of the two layers, the substrate exhibited a high porosity, whereas the zirconia layer was dense with a small amount of closed porosity.

2.3.2.4. Transfer printing

This method involves screen-printing a ceramic organic-based suspension onto a soluble gum paper and drying this layer. Subsequently, an acrylic resin covercoat is screen-printed over the electrolyte layer.

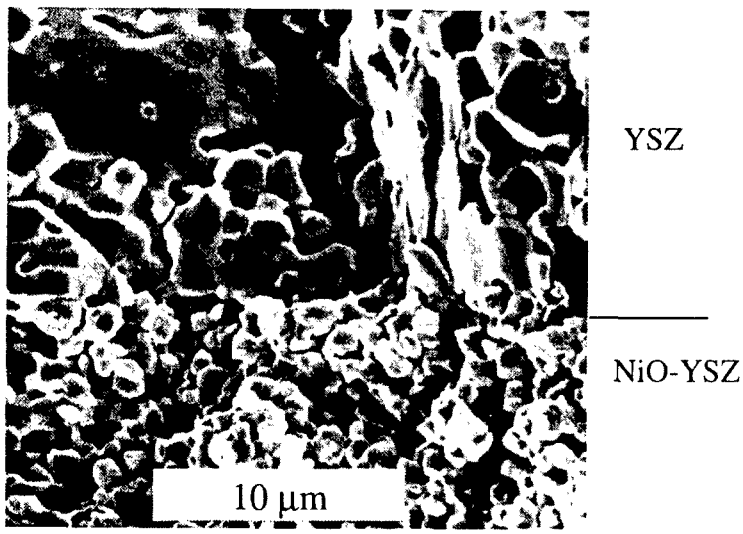

Fig. 12. SEM micrograph of a zirconia layer processed via electrophoretic deposition after sintering. Fracture surface: zirconia on top, Ni–cermet substrate below [117].

The electrolyte layer with the covercoat is released from the gum paper by immersion in water, which dissolves the gum. The layer with the covercoat is then squeezed over the appropriate substrate, dried and fired to full density.

Prica et al. [118] applied this method to fabricate a 1.2-mm layer of yttria-stabilized zirconia electrolyte deposited onto a cermet tube. An OCV of 0.95 V was reached at 1000°C. Will [106] applied transfer printing of zirconia layers on pre-sintered Ni–cermet tapes. A micrograph of the sintered bilayer is shown in Fig. 13.

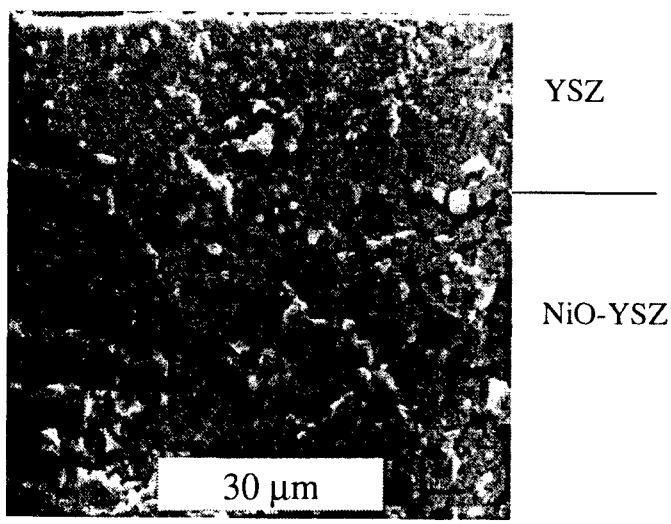

Fig. 13. SEM micrograph of a zirconia layer processed via transfer printing after sintering. Fracture surface: zirconia layer on top, Ni–cermet substrate below [106].

3. Summary and conclusions

This survey shows that many methods for depositing thin and dense YSZ films on dense or porous substrates exist that are based on ceramic powder techniques or chemical and physical processes. These techniques mainly differ in deposition rates, substrate temperature during deposition, precursor materials, necessary equipment, expenditure, and in the quality of the resulting films. These described methods are compared and classified in Table 1.

Although methods such as CVD and PVD are well

Table 1
Comparison of the methods for producing thin and dense electrolytes for SOFC applications

Technique	Film characteristics		Process features	
	Microstructure	Deposition rate or thickness	Cost	Characteristics and limitations
Vapor phase				
Thermal spray technologies		100–500 μm h^{-1}		High deposition rates, various compositions possible, thick and porous coatings, high temperatures necessary
EVD	Columnar structures	3–50 μm h^{-1}	Expensive equipment and processing costs	High reaction temperatures necessary, corrosive gases
CVD	Columnar structures	1–10 μm h^{-1}	Expensive equipment	Various precursor materials possible, high reaction temperatures necessary, corrosive gases
PVD (RF and magnetron sputtering)	Columnar structures	0.25–2.5 μm h^{-1}	Expensive equipment	Tailor-made films, dense and crack-free films, low deposition temperatures, multipurpose technique, relatively small deposition rate
Laser ablation			Expensive equipment (laser)	Intermediate deposition temperatures, difficult upscaling, time-sharing of laser, relatively small deposition rate
Spray pyrolysis	Amorphous to polycrystalline	5–60 μm h^{-1}	Economical	Robust technology, upsealing possible, easy control of parameters, corrosive salts, post-thermal treatment usually necessary
Liquid phase				
Sol-gel, Liquid precursor route	Polycrystalline	0.5–1 μm for each coating	Economical	Various precursors possible, very thin films, low temperature sintering, coating and drying/heating processes have to be repeated 5–10 times, crack formation during drying, many process parameters
Solid phase				
Tape casting	Polycrystalline slightly textured	25–200 μm		Robust technology, upscaling possible, crack formation
Slip casting and slurry coating	Polycrystalline	25–200 μm	Economical	Robust technology, crack formation, slow
Tape calendering	Polycrystalline	5–200 μm		Upscaling possible, co-calendering possible
EPD	Polycrystalline	1–200 μm		Short formation time, little restriction to shape of substrate, suitable for mass production, high deposition rates, inhomogeneous thickness
Transfer printing	Polycrystalline	5–100 μm	Economical	Robust technology, rough substrate surfaces possible, adhesion on smooth substrates difficult
Screen printing	Polycrystalline	10–100 μm	Economical	Robust technology, upscaling possible, crack formation

established, only simple stoichiometric compounds can be deposited, as each component has to be evaporated at different temperatures due to their different vapor pressures. The constituents have to be deposited from independently controlled sources, which add complexity to the system. Ceramic powder methods on the other hand have the potential to be good candidates for complicated stoichiometric compositions or for mixtures of materials.

It is assumed that CVD/EVD and spray pyrolysis will become key technologies for depositing thin electrolyte layers. The investment cost for the CVD apparatus is high [119] compared to droplet and powder techniques whereas the set-up for the spray pyrolysis is inexpensive and simple. This latter method has advantages of uniform coating of large areas, easy control of deposition rates and film thickness, inexpensive experimental set-up under atmospheric conditions [120]. On the other hand, all liquid precursor methods such as sol–gel, spray pyrolysis and slurry coating, are time-, labor- and energy-intensive because coating and drying/sintering has to be repeated in order to avoid crack-formation. Tape casting, electrophoresis, screen-printing, and transfer printing are considered very cost-effective and promising techniques. Whilst these methods may be appropriate for small area cells, the large shrinkage associated with the removal of polymeric binders and plasticizers in subsequent sintering steps reduces the quality of large (>10 cm ∅) area cells. Moreover, it is often difficult to retain adequate porosity within the supporting electrode structures during the cofiring stage for densification of the thick film electrolytes.

References

[1] H.P. Buchkremer, U. Diekmann, L.G.J. de Haart, H. Kabs, U. Stimming, D. Stöver, in: U. Stimming, S.C. Singhal, H. Tagawa, W. Lehnert (Eds.), Proc. 5th Int. Conf. Solid Oxide Fuel Cells, Electrochemical Society, Pennington, NJ, 1997, p. 160.

[2] B.C. Steele, in: U. Bossel (Ed.), Proc. 1st European Solid Oxide Fuel Cell Forum, European SOFC Forum, Oberrohrdorf, Switzerland, 1994, p. 375.

[3] K. Krist, J.D. Wright, in: S.C. Singhal, H. Iwahara (Eds.), Proc. 3rd Int. Symp. on Solid Oxide Fuel Cells, Electrochemical Society, Pennington, NJ, 1993, p. 782.

[4] L.G.J. de Haart, Th. Hauber, K. Mayer, U. Stimming, in: B. Thorstensen (Ed.), Proc. 2nd European Solid Oxide Fuel Cell Forum, European SOFC Forum, Oberrohrdorf, Switzerland, 1996, p. 229.

[5] N.Q. Minh, K. Montgomery, in: U. Stimming, S.C. Singhal, H. Tagawa, W. Lehnert (Eds.), Proc. 5th Int. Conf. Solid Oxide Fuel Cells, Electrochemical Society, Pennington, NJ, 1997, p. 153.

[6] K. Honegger, B. Batawi, Ch. Sprecher, R. Dietheim, in: U. Stimming, S.C. Singhal, H. Tagawa, W. Lehnert (Eds.), Proc. 5th Int. Conf. Solid Oxide Fuel Cells, Electrochemical Society, Pennington, NJ, 1997, p. 321.

[7] J. Schoonman, J.P. Dekker, J.W. Briers, N.J. Kiwiet, Solid State Ionics 46 (1991) 299.

[8] S. de Souza, S.J. Visco, L.C. de Jonghe, in: B. Thorstensen (Ed.), Proc. 2nd European Solid Oxide Fuel Cell Forum, European SOFC Forum, Oberrohrdorf, Switzerland, 1996, p. 677.

[9] N.Q. Minh, T.R. Armstrong, J.R. Esopa, J.V. Guiheen, C.R. Home, F.S. Liu, T.L. Stillwagon, J.J. Van Ackeren, in: F. Gross, P. Zegers, S.C. Singhal, O. Yamamoto (Eds.), Proc. 2nd Int. Symp. on Solid Oxide Fuel Cells, Commission of the European Communities, 1991, p. 93.

[10] N.Q. Minh, K. Montgomery, in: U. Stimming, S.C. Singhal, H. Tagawa, W. Lehnert (Eds.), Proc. 5th Int. Conf. Solid Oxide Fuel Cells, Electrochemical Society, Pennington, NJ, 1997, p. 153.

[11] H. Yamane, T. Hirai, J. Mater. Sci. Lett. 6 (1987) 1229.

[12] H. Yamane, T. Hirai, J. Cryst. Growth 94 (1989) 880.

[13] A.C. Jones, Chem. Vap. Deposition 4 (1998) 169.

[14] Y. Takahashi, T. Kawae, M. Nasu, J. Cryst. Growth 74 (1986) 409.

[15] K.-W. Chour, H. Chen, R. Xu, Thin Solid Films 304 (1997) 106.

[16] M. Aizawa, C. Kobayashi, H. Yamane, T. Hirai, J. Ceram. Soc. Jpn. 101 (1993) 283.

[17] D.A. Glocker, S.I. Shah (Eds.), Handbook of Thin Film Process Technology, Institute of Physics Publishing, 1995.

[18] A.O. Isenberg, in: J.D.E. McIntyre, S. Srinsvan, F.G. Will (Eds.), Proc. Symp. Electrode Materials Processes for Energy Conversion and Storage, Vol. 77, Electrochemical Society, Pennington, NJ, 1977, p. 572.

[19] U. Pal, S.C. Singhal, J. Electrochem. Soc. 137 (1990) 2937.

[20] Y.-S. Lin, Chemical and electrochemical vapor deposition of zirconia–yttria solid solutions in porous ceramic media, Ph.D. Thesis, University of Twente, The Netherlands, 1992.

[21] J.P. Dekker, V.E.J. van Dieten, J. Schoonman, Solid State Ionics 51 (1992) 143.

[22] L.G.J. de Haart, Y.S. Lin, K.J. de Vries, A.J. Burggraaf, Solid State Ionics 47 (1991) 331.

[23] Z. Ogumi, Y. Uchimoto, Y. Tsuji, Z. Takehara, J. Appl. Phys. 72 (1992) 1577.

[24] Z. Ogumi, Y. Uchimoto, Y. Tsuji, Z. Takehara, Solid State Ionics 58 (1992) 345.

[25] J.P. Dekker, P.J. van der Put, R.R. Nieuwenhuis, H.J. Veringa, J. Schoonman, in: Proc. Euro-CVD, Glasgow, Scotland, 1991.

[26] V.E.J. van Dieten, J. Schoonman, Solid State Ionics 57 (1992) 141.
[27] J.L. Deschanvres, F. Cellier, G. Delabouglise, M. Labeau, M. Langlet, J.C. Joubert, J. Appl. Phys. C5 (1989) 695.
[28] T. Ioroi, Y. Uchimoto, Z. Ogumi, Z.I. Takehara, in: M. Dokiya, O. Yamamoto, H. Tagawa, S.C. Singhal (Eds.), Proc. 4th Int. Symp. Solid Oxide Fuel Cells, Vol. 95-1, Electrochemical Society, Pennington, NJ, 1995, p. 603.
[29] A.O. Isenberg, in: Proc. ECS Symp. Electrode Materials, Processes for Energy Conversion and Storage, Vol. 77-6, 1977, p. 963.
[30] G.-Z. Cao, H.W. Brinkman, J. Meijerink, K.J. de Vries, A.J. Burggraaf, J. Am. Ceram. Soc. 76 (9) (1993) 2201.
[31] H. Sasaki, S. Otoshi, M. Suzuki, T. Sogi, A. Kajimura, N. Sugiuara, M. Ippommatsu, Solid State Ionics 72 (1994) 253.
[32] K. Nord-Varhaug, C.H. Chen, E.M. Kelder, F.P.F. van Berkel, J. Schoonman, in: B. Thorstensen (Ed.), Proc. 2nd European Solid Oxide Fuel Cell Forum, European SOFC Forum, Oberrohrdorf, Switzerland, 1996, p. 333.
[33] R.C. Mehrotra, J. Non-Cryst. Solids 100 (1988) 1.
[34] D. Ganguli, D. Kundu, J. Mater. Sci. Lett. 3 (1984) 503.
[35] D. Kundu, P.K. Biswas, D. Ganguli, J. Thin Solid Films 163 (1988) 273.
[36] P. Peshev et al., Mat. Res. Bull. 27 (1992) 1269.
[37] P. Papet et al., J. Mat. Sci. 24 (1989) 3850.
[38] T.W. Kueper, S.J. Visco, L.C. De Jonghe, Solid State Ionics 52 (1992) 251.
[39] C. Sakurai, T. Fukui, M. Okuyama, J. Am. Ceram. Soc. 76 (1993) 1061.
[40] K. Yamada, T.Y. Chow, T. Horihata, M. Nagata, J. Non-Cryst. Solids 100 (1989) 316.
[41] E. Kato, M. Ezoe, K. Daimon, in: S. Somiya, N. Yamamoto, H. Yanagida (Eds.), Science and Technology of Zirconia III, Proc. Advances in Ceramics, Vol. 24, American Ceramic Society, Westerville, OH, 1988, p. 975.
[42] P. Papet, J. Mat. Sci. 24 (1989) 3850.
[43] C.J. Brinker, A.J. Hurd, K.J. Ward, in: L.L. Hench, D.R. Ulrich (Eds.), Ultrastructure Processing of Advanced Ceramics, Wiley, New York, 1988, p. 223.
[44] A.J. Hurd, C.J. Brinker, in: B.J.J. Zelinski, C.J. Brinker, D.E. Clark, D.R. Ulrich (Eds.), Better Ceramics through Chemistry, Vol. IV, North-Holland, New York, 1990, p. 575.
[45] C.J. Brinker, G.W. Scherer, Sol-Gel Science, Academic Press, New York, 1990.
[46] W.J. Daughton, S.L. Givens, J. Electrochem. Soc. 129 (1982) 173.
[47] K. Mehta, R. Xu, Y.V. Virkar, J. Sol-Gel Science and Technology 11 (1998) 203.
[48] S.W. Nam, S.-G. Kim, S.-P. Yoon, S.-A. Hong, S.-H. Hyun, in: Proc. Fuel Cell Seminar, Palm Springs, Nov. 16–19, 1998, p. 60.
[49] C.C. Chen, M.M. Nasrallah, H.U. Anderson, Solid State Ionics 70/71 (1994) 101.
[50] H.U. Anderson, C.C. Chen, M.M. Nasrallah, Method of coating a substrate with a metal oxide film from an aqueous solution comprising a metal cation and a polymerizable organic solvent, US Patent No. 5,494,700, February 27, 1996.
[51] C. Reiichi, Y. Fumikatsu, Y. Junichi, in: Proc. MRS Fall Meeting, 496, Warrendale, PA, 1998, p. 181.
[52] K.L. Choy, in: W.E. Lee (Ed.), British Ceramic Proc., Vol. 54, 1995, p. 65.
[53] H. Ruiz, H. Vesteghem, A.R. Di Giampaolo, J. Lira, J. Surface and Coatings Technology 89 (1997) 77.
[54] J.L. Deschanvres et al., J. de Physique 50 (1989) 695.
[55] C.H. Chen, K. Nord-Varhaug, J. Schoonman, J. Mater. Synthesis and Processing 4 (1996) 189.
[56] T. Setoguchi, M. Sawano, K. Eguchi, H. Arai, Solid State Ionics 40–41 (1990) 502.
[57] D. Perednis, unpublish. results, Department of Materials, Nonmetallic Materials, ETH, Zurich, 1998.
[58] A.J. Sturgeon, Materials World June (1993) 351.
[59] L.W. Tai, P.A. Lessing, J. Am. Ceram. Soc. 74 (1991) 501.
[60] D.J. Varcalle Jr., G.R. Smolik, G.C. Wilson, G. Irons, J.A. Walter, Mater. Res. Soc. Symp. Proc. 155 (1989).
[61] G.M. Ingo Am., J. Am. Ceram. Soc. 74 (1991) 381.
[62] P.D. Harmsworth, R. Stevens, J. Mater. Sci. 27 (1992) 616.
[63] M. Scagliotti, F. Parmigiani, G. Samoggia, G. Lanzi, D. Richon, J. Mater. Sci. 23 (1988) 3764.
[64] T. Setoguchi, K. Eguchi, H. Arai, J. Vacuum 46 (1991) 1601.
[65] H. Arai, K. Eguchi, T. Setoguchi, R. Yamaguchi, in: S.C. Singhal, H. Iwahara (Eds.), Proc. 3rd Int. Conf. Solid Oxide Fuel Cells, Electrochemical Society, Pennington, NJ, 1991, p. 167.
[66] A.R. Nicoll, A. Salito, K. Honegger, Solid State Ionics 52 (1992) 269.
[67] G. Schiller, R. Henne, M. Lang, in: U. Stimming, S.C. Singhal, H. Tagawa, W. Lehnert (Eds.), Proc. 5th Int. Conf. Solid Oxide Fuel Cells, Electrochemical Society, Pennington, NJ, 1997, p. 635.
[68] Y. Aihara, S. Ito, S. Kawasaki, in: M. Dokiya, O. Yamamoto, H. Tagawa, S.C. Singhal (Eds.), Proc. 4th Int. Conf. Solid Oxide Fuel Cells, 1995, p. 180.
[69] R. Henne, E. Fendler, M. Lang, in: U. Bossel (Ed.), Proc. 1st European Solid Oxide Fuel Cell Forum, European SOFC Forum, Oberrohrdorf, Switzerland, 1994, p. 617.
[70] H.R. Gruner, H. Tannenberger, in: U. Bossel (Ed.), Proc. 1st European Solid Oxide Fuel Cell Forum, European SOFC Forum, Oberrohrdorf, Switzerland, 1994, p. 611.
[71] A. Ahmed, E. Ahmed, Materials World June (1993) 344.
[72] P.T. Murray, J.D. Wolf, J.A. Meseher, J.T. Grant, N.T. McDevitt, J. Mater. Lett. 5 (1987) 250.
[73] F. Kokai, K. Amano, H. Ota, F. Umemura, J. Appl. Phys. A54 (1992) 340.
[74] F. Kokai, K. Amano, H. Ota, Y. Ochiai, F. Umemura, J. Appl. Phys. 72 (1992) 699.
[75] K.M. Jasim, R.D. Rawlings, D.R.F. West, J. Mat. Sci. 26 (1991) 909.
[76] K.M. Jasim, R.D. Rawlings, D.R.F. West, J. Mat. Sci. 27 (1992) 3903.
[77] K. Tsukamoto, F. Uchiyama, Y. Ohno, Y. Kage, Surface Eng. 6 (1990) 45.
[78] K. Tsukamoto et al., Solid State Ionics 40/41 (1990) 1003.
[79] Y. Miyahara, J. Appl. Phys. 71 (1992) 2309.
[80] C.R. Aita, H.-K. Kwok, J. Am. Ceram. Soc. 73 (1990) 3209.

[81] K. Nakagawa, H. Yohioka, C. Kuroda, M. Ishida, Solid State Ionics 35 (1989) 249.
[82] J.A. Thornton, J. Vac. Sci. Technol. 11 (1974) 666.
[83] F.A. Smidt, Int. Mater. Rev. 35 (1990) 61.
[84] H. Michibata, T. Namikawa, Y. Yamazaki, Denki Kagaku 58 (11) (1990) 1070.
[85] K. Mehta, S.J. Hong, J.-F. Jue, A.V. Virkar, in: S.C. Singhal, H. Iwahara (Eds.), Proc 3rd Int. Symp. on Solid Oxide Fuel Cells, Electrochemical Society, Pennington, NJ, 1993, p. 92.
[86] P. Charpentier, P. Fragnaud, D.M. Schleich, C. Lunot, in: U. Stimming, S.C. Singhal, H. Tagawa, W. Lehnert (Eds.), Proc. 5th Int. Conf. Solid Oxide Fuel Cells, Electrochemical Society, 1997, p. 1169.
[87] Q.-H. Gao, R.E. Rocheaeau, B.Y. Liaw, in: S.C. Singhal, H. Iwahara (Eds.), Proc. 3rd Int. Conf. Solid Oxide Fuel Cells, Electrochemical Society, Pennington, NJ, 1993, p. 38.
[88] F. Konushi et al., in: J.M. Gibson, G.C. Osborn, R.M. Tromp (Eds.), Layered Structures and Epitaxy, Materials Research Society, Pittsburgh, 1985, p. 259.
[89] F. Jones, J. Vac. Sci. Technol. 6 (1988) 3088.
[90] L.S. Wang, S.A. Barnett, J. Electrochem. Soc. 139 (1992) 1134.
[91] L.S. Wang, S.A. Barnett, Solid State Ionics 61 (1993) 273.
[92] K. Honegger, E. Batawi, Ch. Sprecher, R. Diethelm, in: U. Stimming, S.C. Singhal, H. Tagawa, W. Lehnert (Eds.), Proc. 5th Int. Conf. Solid Oxide Fuel Cells, Electrochemical Society, 1997, p. 321.
[93] P.K. Srivastava et al., in: B. Thorstensen (Ed.), Proc. 2nd European Solid Oxide Fuel Cell Forum, European SOFC Forum, Oberrohrdorf, Switzerland, 1996, p. 761.
[94] C. Kleinlogel, M. Gödickemeier, K. Honegger, L.J. Gauckler, in: H.L. Tuller, A.C. Khandkar, M. Mogensen, W. Gopel (Eds.), Proc. Ionic and Mixed Conducting Ceramics, Vol. III, Electrochemical Society, Pennington, NJ, 1997, p. 97.
[95] T. Hikita, M. Kawashima, I. Yasuda, T. Koyama, Y. Matsuzaki, in: S.C. Singhal, H. Iwahara (Eds.), Proc. 3rd Int. Symp. on Solid Oxide Fuel Cells, Electrochemical Society, Pennington, NJ, 1993, p. 714.
[96] R. Diethelm, K. Honegger, in: S.C. Singhal, H. Iwahara (Eds.), Proc. 3rd Int. Symp. on Solid Oxide Fuel Cells, Electrochemical Society, Pennington, NJ, 1993, p. 822.
[97] W.F. Chu, Solid State Ionics 52 (1992) 243.
[98] D. Bauza, D. Especel, M. Gouet, British Ceramic Proc. 38 (1986) 197.
[99] M. Gödickemeier, unpublished results, Department of Materials, Nonmetallic Materials, ETH, Zurich, 1993.
[100] M. Cassidy, G. Lindsay, in: U. Bossel (Ed.), Proc. 1st European Solid Oxide Fuel Cell Forum, European SOFC Forum, Oberrohrdorf, Switzerland, 1994, p. 617.
[101] M. Cassidy, K. Kendall, C. Lindsay, in: B. Thorstensen (Ed.), Proc. 2nd European Solid Oxide Fuel Cell Forum, European SOFC Forum, Oberrohrdorf, Switzerland, 1996, p. 667.
[102] B.H. Rabin, J. Am. Ceram. Soc. 73 (1990) 2757.
[103] D.W. Dees, T.D. Claar, T.E. Easler, D.C. Fee, F.C. Mrazek, J. Electrochem. Soc. 134 (1987) 2141.
[104] F.P.F. van Berkel, G.M. Christie, F.H. van Heuveln, J.P.P. Huijsmans, in: M. Dokiya, O. Yamamoto, H. Tagawa, S.C. Singhal (Eds.), Proc. 4th Int. Conf. Solid Oxide Fuel Cells, 1995, p. 1062.
[105] R. Ihringer, J. Van Herle, A.J. McEvoy, in: U. Stimmung, S.C. Singhal, H. Tagawa, W. Lehnert (Eds.), Proc. 5th Int. Conf. Solid Oxide Fuel Cells, Electrochemical Society, Pennington, NJ, 1997, p. 340.
[106] J. Will, Porous support structures and sintered thin film electrolytes for solid oxide fuel cells, Diss. ETH No. 12876, ETH, Zurich, 1998.
[107] H. Arai, in: S.C. Singhal (Ed.), Proc. 1st Int. Symp. on Solid Oxide Fuel Cells, Electrochemical Society, Pennington, NJ, 1989, p. 10.
[108] M. Aizawa, H. Nishiyama, A. Ueno, M. Kuroishi, K. Eguchi, H. Arai, in: S.C. Singhal, H. Iwahara (Eds.), 3rd Int. Symp. on SOFC, Electrochemical Society, Pennington, NJ, 1993, p. 38.
[109] S.K. Nam, W.S. Seong, S.A. Hong, in: M. Dokiya, O. Yamamoto, H. Tagawa, S.C. Singhal (Eds.), Proc. 4th Int. Conf. Solid Oxide Fuel Cells, 1995, p. 318.
[110] S.J. Visco, S. de Souza, L.C. De Jonghe, in: Proc. EPORI/GRI Fuel Cell Workshop on Fuel Cell Technology Research and Development, April 4–5, 1995, p. 15.
[111] S. de Souza, S.J. Visco, L.C. de Jonghe, J. Electrochem. Soc. 144 (3) (1997) L35.
[112] T. Setoguchi, T. Inoue, H. Takebe, E. Eguchi, K. Morinaga, H. Arai, Solid State Ionics 37 (1990) 217.
[113] T. Setoguchi, K. Okamoto, K. Eguchi, H. Arai, J. Electrochem Soc. 139 (1992) 2875.
[114] R. Förthmann, G. Blaß, H.P. Buchkremer, in: U. Stimming, S.C. Singhal, H. Tagawa, W. Lehnert (Eds.), Proc. 5th Int. Conf. Solid Oxide Fuel Cells, Electrochemical Society, Pennington, NJ, 1997, p. 1003.
[115] P. Sarkar, P.S. Nicholson, J. Am. Ceram. Soc. 79 (8) (1996) 1987.
[116] T. Ishihara, K. Sato, Y. Takita, J. Am. Ceram. Soc. 79 (4) (1996) 913.
[117] M. Hruschka, Entwicklung der Elektrophoretischen fur die Herstellung dunner Elektrolytschichten, Ph.D. Thesis, University of Aachen, Berichte des Forschungszentrum Jülich, Germany, 1996.
[118] M. Prica, K. Kendall, M. Painter, in: M. Dokiya, O. Yamamoto, H. Tagawa, S.C. Singhal (Eds.), Proc. 4th Int. Conf. Solid Oxide Fuel Cells, 1995, p. 1056.
[119] H. Itoh, M. Mon, N. Mori, T. Abe, J. Power Sources 49 (1994) 315.
[120] M.H. Francombe, J.L. Vossen, in: Physics of Thin Films, Academic Press, NJ, 1982, p. 230.